



# Circular Dichroism in the Photoelectron Angular Distributions of Camphor and Fenchone from Multiphoton Ionization with Femtosecond Laser Pulses\*\*

Christian Lux, Matthias Wollenhaupt, Tom Bolze, Qingqing Liang, Jens Köhler, Cristian Sarpe, and Thomas Baumert\*

Chiral recognition in the gas phase using light is a challenge because of the low particle densities involved. However, such collision free conditions offer great promise for highly sensitive analytical applications as well as for unraveling fundamental aspects of the light–matter interaction.<sup>[1]</sup> Often ionizing radiation is used for such investigations, as charged particles offer nearly unit detection efficiencies. In addition, highly differential detection schemes have been developed to measure the photoelectron angular distribution (PAD), which contains rich information about the photoionization dynamics and intramolecular dynamics.<sup>[2]</sup> An efficient and relatively simple method to measure the three-dimensional PAD is to project the complete distribution onto a two-dimensional detector plane. The so-called velocity map imaging technique<sup>[3]</sup> (VMI) is a prominent example of this approach. Based on certain symmetry assumptions concerning the PAD, the three-dimensional PAD can be reconstructed from the two-dimensional image by inversion techniques, as for example, described in Ref. [4]. If there are no symmetries in the PAD, tomographic reconstruction methods have been employed.<sup>[5]</sup> More sophisticated coincidence techniques are available, for instance, when PADs from the molecular frame of dissociating molecules are of interest.<sup>[6,7]</sup>

Making use of vacuum ultraviolet (VUV) synchrotron ionization, a striking forward/backward asymmetry in the electron ejection with respect to the light propagation was found in one-photon ionization of randomly oriented small chiral molecules with circularly polarized light<sup>[8–10]</sup> and reviewed in chapter one of Ref. [1] by Nahon and Powis and also in Ref. [11]. This effect was termed photoelectron circular dichroism (PECD) and, based on theoretical predictions,<sup>[12]</sup> was attributed to an electric dipole interaction<sup>[11]</sup> PECD shows a effect several orders larger than that of conventional circular dichroism (CD) techniques and is therefore attractive for chiral recognition in the gas phase.

A wide-spread implementation of this effect in analytics has been hampered to date as the use of a synchrotron facility to deliver the required radiation seems to be a prerequisite.


Herein we show, that PECD is also accessible using femtosecond laser pulses from a standard setup. We make use of resonance enhanced multiphoton ionization (REMPI) and measure PAD images from randomly oriented chiral molecules with a VMI setup. Camphor and fenchone were chosen as prototypes, as these molecules have also been used in benchmark experiments on normal CD as well as in the pioneering work on PECD using VUV one-photon ionization and VMI detection.<sup>[13]</sup>

PADs from one-photon ionization of randomly oriented molecules in the laboratory frame can be expanded in Legendre polynomials  $P_l(\cos\theta)$  where the energy distribution can be accounted for by a sum of Gaussians and  $\theta$  is the angle of the ejected electron with respect to the direction of light propagation for the circularly polarized light.<sup>[4]</sup> Expressions for multiphoton ionization with different polarizations can be found for example in Refs. [2, 14, 15]. PECD in VUV one-photon ionization manifests itself in a change of sign of the first-order Legendre polynomial when changing from left-circularly polarized light (LCP) to right-circularly polarized light (RCP) when a specific enantiomer is ionized. A change of sign is also obtained by keeping the helicity of the light and changing from the *S* to the *R* enantiomer. In our case we ionize with three photons out of the highest occupied orbital of the neutral molecules. The ionization is enhanced by a resonance after the absorption of two photons (2+1 REMPI). In our measured PAD images, we find asymmetries in all the contributing odd Legendre polynomials up to the seventh order when changing the helicity or when changing from the *S* to the *R* enantiomers but keeping the helicity. Looking at the PECD effect obtained by subtraction of the RCP image from the LCP image measured on one specific enantiomer we find a complete asymmetry in the corresponding odd Legendre polynomials. The effect is in the  $\pm 10\%$  regime on both substances studied and is even clearly visible in the difference of the raw data. In the following we will first briefly address our experimental approach followed by our data evaluation procedure including discussion before we conclude.

The experimental setup is shown in Figure 1a and the polarization characterization is shown in Figure 1b. Details are given in the Supporting Information. Camphor and fenchone were purchased at Sigma–Aldrich with an enantiomeric purity of over 95%. The 2+1 REMPI<sup>[17]</sup> scheme is

[\*] C. Lux, Prof. Dr. M. Wollenhaupt, T. Bolze, Dr. Q. Liang, J. Köhler, C. Sarpe, Prof. Dr. T. Baumert  
Institut für Physik und Center for Interdisciplinary Nanostructure Science and Technology (CINSaT), Universität Kassel  
Heinrich-Plett-Strasse 40, 34132 Kassel (Germany)  
E-mail: tbaumert@uni-kassel.de  
Homepage: <http://www.physik.uni-kassel.de/exp3.html>

[\*\*] Financial support by the EU ITN FASTQUAST and the DFG is gratefully acknowledged. We also thank Manuel Gerlach for help in the initial stage of the project.

 Supporting information for this article is available on the WWW under <http://dx.doi.org/10.1002/anie.201109035>.

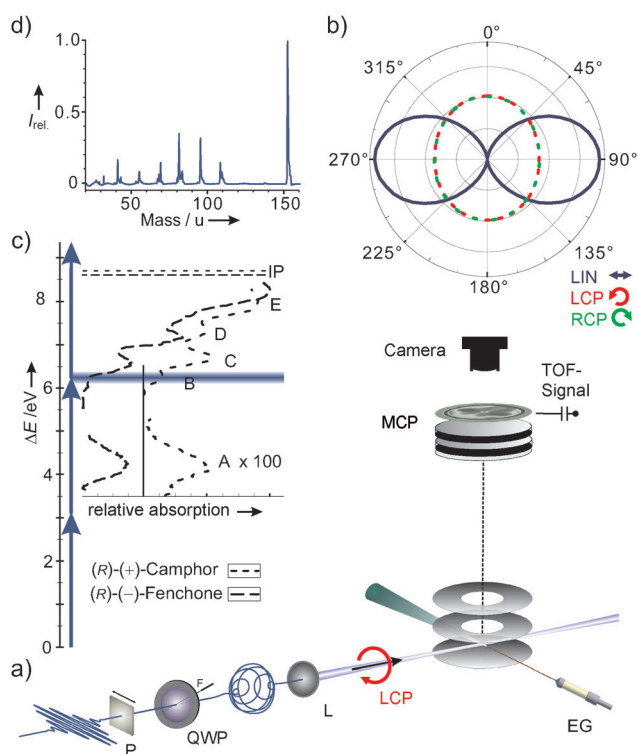


**Figure 1.** a) Experimental setup with beam path, spectrometer, and multichannel plate (MCP) detector: Laser pulses with a pulse duration of 25 fs centered at 398 nm are focused into an energy-calibrated imaging spectrometer.<sup>[16]</sup> An average laser power of 2.5 mW at 1 kHz repetition rate results in a peak intensity  $I_0$  of about  $5 \times 10^{13} \text{ W cm}^{-2}$ . The spectrometer is used to record images of PADs and also ion time-of-flight (TOF) spectra. P: polarizer, QWP: quarter wave plate to generate either LCP or RCP light (F: fast axis), L: lens, EG: effusive gas inlet. b) Degree of polarization for linearly (LIN) and circularly polarized (LCP and RCP) laser pulses. The Stokes parameter  $S_3$  for the circularly polarized light is  $|S_3| = 99\%$ . c) Excitation and ionization scheme of camphor and fenchone adapted from Ref. [18] and IPs taken from Refs. [13, 19]. A–E are labels for absorption bands. d) Typical ion TOF spectrum for (S)-(-)-camphor using left-circularly polarized light.

depicted in Figure 1c where the region of the B band<sup>[18]</sup> acts as the resonant intermediate state. The vertical ionization potential (IP) of camphor is 8.7 eV<sup>[19]</sup> and 8.6 eV<sup>[13]</sup> for fenchone. The total energy for three photons from our laser is about 9.35 eV, thus ionization can only occur from the highest occupied orbital.<sup>[13, 19]</sup> The Keldysh  $\gamma$  parameter at  $I_0$  is larger than two, indicating a multiphoton regime. Measured power laws ranging from  $0.3 I_0$  to  $1.2 I_0$  on the photoelectron yield for all polarizations in an energy interval from approximately 0.02 to 0.78 eV gave a multiphoton exponent of about 3 for fenchone and 2.2 to 2.5 for camphor, supporting the 2+1 excitation scheme although the results for camphor indicate the onset of saturation effects. The low-energy photoelectrons below 0.02 eV did not stem from residual gas and showed a power-law exponent about 0.5 larger than the numbers given above indicating the occurrence of ionization processes. This contribution is thus not included in the data analysis. A typical ion time-of-flight (TOF) spectrum for (S)-(-)-camphor using LCP light at  $I_0$  is displayed in Figure 1d. Note that

the spectrum is dominated by the parent ion at 152 atomic units. With decreasing intensity we observe that the relative parent-ion yield increases with respect to the fragments at lower masses. This is a typical behavior for dissociative ionization, that is, ionization precedes fragmentation.<sup>[20]</sup> That the process is dissociative ionization is also supported by the measured and analyzed PAD images as they do not change their shape as a function of intensity. The CD effect in the ion yield—as observed on chiral molecules when dedicated REMPI schemes are employed using nanosecond<sup>[21, 22]</sup> or femtosecond<sup>[23, 24]</sup> laser sources in the visible and near UV—was not detectable under our experimental conditions on camphor and fenchone.

We now turn to the main result of our experiment, that is, the large PECD effect. PAD images from camphor and fenchone for differently polarized laser pulses are shown in Figure 2. All the PAD images were obtained under the experimental conditions described above (detailed in the Supporting Information) and averaged over the same number of laser pulses (665 000). To eliminate potential small drifts in the setup, a fast stepper motor was used to rotate the quarter wave plate (QWP) to switch between RCP and LCP measurements back and forth 100 times (i.e. every 6650 pulses). A 2D Fourier filter was applied to the  $1024 \times 1024$  pixels image to remove high-frequency noise. Differences in the total signal (excluding the low energy part, i.e. that under 0.02 eV) for RCP measurements compared to LCP measurements were within a range of 0.5%. The PAD images were normalized to the corresponding total signal and finally—to facilitate comparison—a scaling factor was defined for camphor and another for fenchone. This scaling factor was applied to all the data within one set and chosen so that the region with the highest signal in the RCP and LCP PAD images corresponds to unity in the color coding. The top row in Figure 2a shows PAD images for (R)-(+)-camphor resulting from ionization with LIN, LCP, and RCP light. The laser propagation is from left to right as indicated with the arrow. For ionization with LIN light the PAD image is symmetric with respect to the light propagation. A perpendicular line through the center of the PAD image is the mirror axis and coincides with the direction of the linear polarization. In contrast, the PAD image resulting from ionization with LCP light exhibits an asymmetry with respect to the light propagation: more signal is observed in the forward direction than the backward direction. The opposite result is obtained by ionization with RCP light, with more signal found in the backward direction than the forward direction. Qualitatively the same behavior is observed in the PAD images on (R)-(-)-fenchone displayed in the top row of Figure 2b. The second row in Figure 2a shows the results when changing from (R)-(+)-camphor to (S)-(-)-camphor. In this case the ionization with LIN light also results in a symmetric PAD image with respect to the light propagation, however, for LCP light more signal is seen in the backward direction and for RCP light more signal is detected in the forward direction. Again the same behavior is seen in the second row of Figure 2b where (R)-(-)-fenchone was exchanged to (S)-(+)-fenchone. This observed change in the PAD images either by mirroring the helicity of the light or by mirroring the molecule is expected

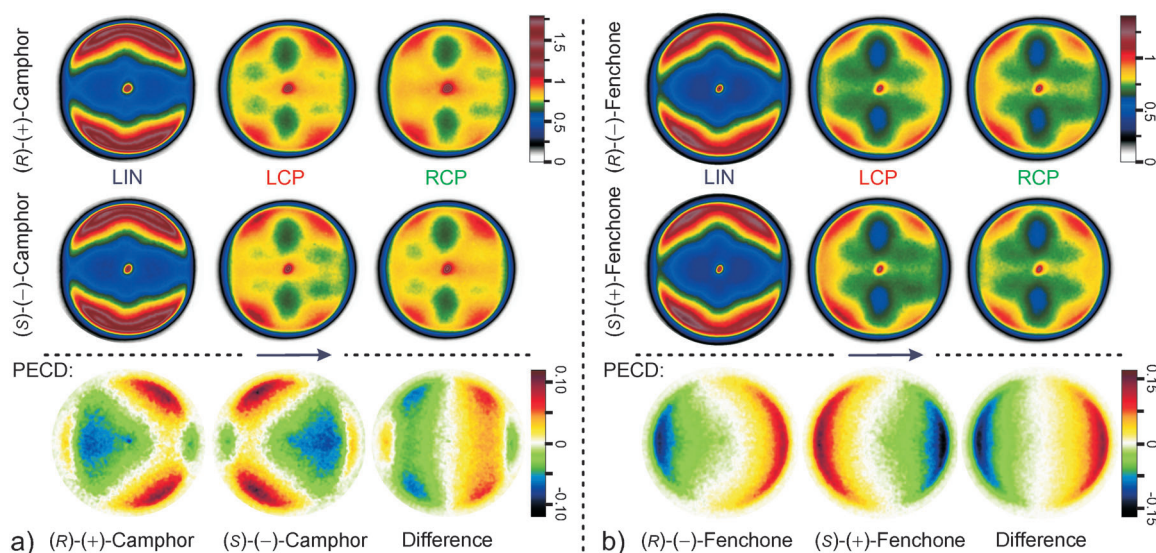


**Figure 2.** a) Top row: PAD images from (R)-(+)-camphor resulting from ionization with LIN, LCP, and RCP light, respectively. The laser propagation as indicated by an arrow is from left to right. For ionization with LIN light the PAD image is symmetric with respect to the light propagation. The PAD image resulting from ionization with LCP light exhibits an asymmetry with respect to the light propagation (more signal in forward direction) whereas for RCP light more signal is observed in the backward direction. Second row: PAD images for (S)-(-)-camphor. Note the change in signal asymmetry in forward/backward direction. Third row, left image: PECD signal—taking LCP-PAD image minus RCP-PAD image—for (R)-(+)-camphor; middle image: PECD signal for (S)-(-)-camphor; note the reversed asymmetry in forward/backward direction on changing the enantiomer; right image: the difference of the PECD signals of the R- and S-enantiomers shows the complete antisymmetry in our experiment by removing residual instrumental asymmetries; for comparison, the numbers in the color scale were multiplied by 0.5 in the latter image. b) Same as (a) for fenchone.

from a CD effect. Because it is already visible in the raw data the effect is significantly larger than other CD effects. In the third row of Figure 2a we plot the PECD signal for (R)-(+)-camphor (left image) and (S)-(-)-camphor (middle image) following the convention suggested by Powis,<sup>[11]</sup> that is, taking the LCP-PAD image minus the RCP-PAD image. The data for fenchone are displayed in the corresponding parts of Figure 2b. Pronounced asymmetries with respect to the forward/backward direction are detected for both molecules, changing direction when changing from right-handed to left-handed molecules. The asymmetries are in the range of  $\pm 10\%$  and slightly larger for fenchone. However, the PECD signals are not perfectly antisymmetric. For a pure PECD effect we expect that only odd Legendre polynomials contribute as only odd Legendre polynomials show antisymmetry with respect to the forward/backward direction, whereas even Legendre polynomials are symmetric with that respect (see left columns of Figure 3). For further details on the symmetry properties of the PECD signals see Figure S1 in the Supporting Information. The residual deviation from complete asymmetry could be due to remaining small differences in the ellipticity for LCP and RCP light. These differences can be removed by subtracting the PECD signal of the S-enantiomer from the PECD signal of the R-enantiomer. The resulting difference of the PECD signals is displayed in Figure 2 (right image of the third row).

Looking at the PECD signals of camphor, the third Legendre polynomial seems to contribute most, whereas for fenchone the first Legendre polynomial is dominant. To obtain quantitative information for the different contributions we performed an Abel inversion assuming a cylindrically

symmetric photoelectron distribution projected onto a two dimensional detector plane where the symmetry axis is the light-propagation axis and is parallel to the detector plane. We employed the pBasex approach,<sup>[4]</sup> to speed up the calculation we downscaled our PAD images shown in Figure 2 to  $200 \times 200$  pixels. Our pBasex algorithm expands a  $\text{PAD}(R, \theta)$  in 100 spherical Gaussian distributions in steps of 2 pixels. Each Gaussian has a width  $\sigma$  of 2 pixels, is centered at  $R_k$  and is multiplied by a sum of 4 even and 4 odd Legendre polynomials. Higher-order Legendre polynomials were considered in addition but did not contribute significantly. The offset is taken care of by the zero-order Legendre polynomial where  $\theta$  is measured with respect to the light propagation [Eq. (1)].

$$\text{PAD}(R, \theta) = \sum_{k, l=0}^{k=100, l=8} c_{kl} e^{-\frac{(R-R_k)^2}{\sigma}} P_l(\cos \theta) \quad (1)$$

The radius  $R$  is proportional to the square root of the kinetic energy in a VMI setup. Abel-inverted and energy-calibrated PAD images for (R)-(+)-camphor are displayed in the top row of Figure 3a and for (R)-(-)-fenchone in the top row of Figure 3b. To visualize the expected antisymmetry we derived the symmetric and the antisymmetric component from the Abel-inverted PECD signal. The antisymmetric part was obtained by subtracting the symmetrized part, obtained by  $180^\circ$  back-folding. An analogous decomposition of the PECD signals from camphor and fenchone is shown in Figure S1 in the Supporting Information. The main contribution to the signal for camphor is centered at an excess energy of approximately 0.52 eV, and for fenchone at approximately



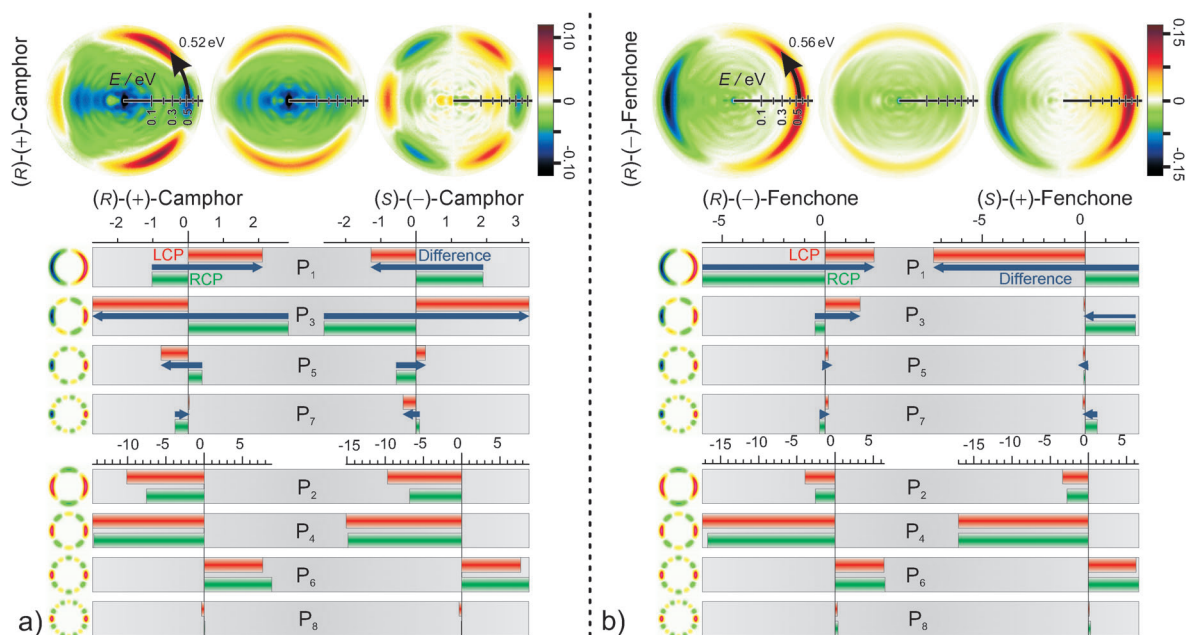


**Figure 3.** a) Upper row: Abel-inverted PECD signal for (R)-(+)-camphor and decomposition into symmetric and antisymmetric components. The main contribution to the photoelectron signal is at 0.52 eV. Lower part: Retrieved averaged Legendre coefficients  $c_{kl}$  from the different orders of Legendre polynomials  $P_l$  schematically shown on the left side. Red bars: LCP amplitudes, green bars: RCP amplitudes. All odd Legendre polynomials change sign either on changing the helicity of the light or the handedness of the molecule (difference indicated with blue arrows) whereas the even contributions do not. b) Same as (a) for fenchone. The maximum of the kinetic energy distribution is at 0.56 eV.

0.56 eV, both with a full-width at half maximum (FWHM) of approximately 0.23 eV. These values are 200 meV lower than expected from the above mentioned vertical ionization potentials from synchrotron experiments but in reasonable agreement considering the 2+1 REMPI process. In addition dynamic resonances can modify the excess energy<sup>[25]</sup> and multiphoton resonances are likely to be shifted by strong fields.<sup>[26]</sup> The involved Legendre coefficients  $c_{kl}$  out of the pBasex are summarized in Figure 3a for camphor and in Figure 3b for fenchone. The coefficients are averaged over about 17 Gaussian basis sets within the FWHM of the kinetic-energy distribution. The expected main contribution of the third Legendre polynomial to the PECD on camphor and the dominance of the first Legendre polynomial in the fenchone data are clearly visible. It is also seen that all odd Legendre polynomials change sign either on changing the helicity of the light whereas the even contributions do not. The coefficients  $c_{kl}$  are tabulated in Table S1 and S2 in the Supporting Information. The reported values are robust within  $\pm 0.3$  (absolute value) with respect to pressure variations between  $1 \times 10^{-6}$  and  $6 \times 10^{-6}$  mbar ruling out contributions from space charge effects and also with respect to intensity variations from  $0.3I_0$  to  $1.2I_0$  ruling out a significant change of ionization processes in this intensity interval. Also no fundamental change of the PECD signal was observed when changing the chirp (i.e. a linear variation of frequency with respect to time) from  $-500 \text{ fs}^2$  to  $+2000 \text{ fs}^2$ . At the highest intensities, electrons with an additional energy of one photon are also observed originating from above threshold ionization (ATI). These ATI electrons also show asymmetries with respect to the forward/backward direction

of the light propagation, however, the low signal-to-noise ratio has so far prevented us from providing quantitative information about this contribution.

In summary we have demonstrated a circular dichroism effect in the  $\pm 10^\circ$  regime derived from images of photoelectron angular distributions resulting from resonance enhanced multiphoton ionization of randomly oriented chiral molecules in the gas phase. Camphor and fenchone were chosen as prototypes. So far this circular dichroism effect was only observed in one-photon ionization experiments at synchrotron facilities. We believe that our table-top laser-based approach opens the door to many analytical applications. In the future we will explore the nuclear and electron dynamics of the intermediate resonance with the help of coherent control techniques.<sup>[27]</sup> In addition to a possible enhancement of the effect, such studies may also help to determine the absolute configuration by comparison with ab initio quantum-dynamic calculations.

Received: December 21, 2011  
Published online: February 20, 2012

**Keywords:** chirality · circular dichroism · femtosecond laser pulses · multiphoton ionization · photoelectron spectroscopy

- [1] A. Zehnacker in *Chiral Recognition in the Gas Phase* (Ed.: A. Zehnacker), CRC, Boca Raton, **2010**.
- [2] K. L. Reid, *Annu. Rev. Phys. Chem.* **2003**, *54*, 397–424.
- [3] A. T. J. B. Eppink, D. H. Parker, *Rev. Sci. Instrum.* **1997**, *68*, 3477–3484.

- [4] G. A. Garcia, L. Nahon, I. Powis, *Rev. Sci. Instrum.* **2004**, *75*, 4989–4996.
- [5] M. Wollenhaupt, M. Krug, J. Köhler, T. Bayer, C. Sarpe-Tudoran, T. Baumert, *Appl. Phys. B* **2009**, *95*, 647–651.
- [6] J. Ullrich, R. Moshhammer, A. Dorn, R. Dörner, L. P. H. Schmidt, H. Schmidt-Böcking, *Rep. Prog. Phys.* **2003**, *66*, 1463–1545.
- [7] A. Vredenburg, W. G. Roeterdink, M. H. M. Janssen, *Rev. Sci. Instrum.* **2008**, *79*, 063108.
- [8] N. Böwering, T. Lischke, B. Schmidtke, N. Müller, T. Khalil, U. Heinzmann, *Phys. Rev. Lett.* **2001**, *86*, 1187–1190.
- [9] G. A. Garcia, L. Nahon, M. Lebech, J.-C. Houver, D. Dowek, I. Powis, *J. Chem. Phys.* **2003**, *119*, 8781–8784.
- [10] S. Turchini, N. Zema, G. Contini, G. Alberti, M. Alagia, S. Stranges, G. Fronzoni, M. Stener, P. Decleva, T. Prospero, *Phys. Rev. A* **2004**, *70*, 014502.
- [11] I. Powis, *Adv. Chem. Phys.* **2008**, *138*, 267–329.
- [12] B. Ritchie, *Phys. Rev. A* **1976**, *13*, 1411–1415.
- [13] I. Powis, C. J. Harding, G. A. Garcia, L. Nahon, *ChemPhysChem* **2008**, *9*, 475–483.
- [14] B. Whitaker in *Imaging in Molecular Dynamics* (Ed.: B. Whitaker), Cambridge University Press, Cambridge, **2003**.
- [15] T. Seidemann, *J. Chem. Phys.* **1997**, *107*, 7859–7868.
- [16] M. Wollenhaupt, M. Krug, J. Köhler, T. Bayer, C. Sarpe-Tudoran, T. Baumert, *Appl. Phys. B* **2009**, *95*, 245–259.
- [17] J. W. Driscoll, T. Baer, T. J. Cornish, *J. Mol. Struct.* **1991**, *249*, 95–107.
- [18] F. Pulm, J. Schramm, J. Hormes, S. Grimme, S. D. Peyerimhoff, *Chem. Phys.* **1997**, *224*, 143–155.
- [19] E. E. Rennie, I. Powis, U. Hergenhahn, O. Kugeler, G. Garcia, T. Lischke, S. Marburger, *J. Electron Spectrosc. Relat. Phenom.* **2002**, *125*, 197–203.
- [20] L. Bañares, T. Baumert, M. Bergt, B. Kiefer, G. Gerber, *J. Chem. Phys.* **1998**, *108*, 5799–5811.
- [21] U. Boesl, A. Bornschlegel, *ChemPhysChem* **2006**, *7*, 2085–2087.
- [22] C. Logé, U. Boesl, *ChemPhysChem* **2011**, *12*, 1940–1947.
- [23] H. G. Breunig, G. Urbasch, P. Horsch, J. Cordes, U. Koert, K.-M. Weitzel, *ChemPhysChem* **2009**, *10*, 1199–1202.
- [24] P. Horsch, G. Urbasch, K.-M. Weitzel, *Z. Phys. Chem.* **2011**, *225*, 587–594.
- [25] A. Assion, T. Baumert, J. Helbing, V. Seyfried, G. Gerber, *Chem. Phys. Lett.* **1996**, *259*, 488–494.
- [26] M. Krug, T. Bayer, M. Wollenhaupt, C. Sarpe-Tudoran, T. Baumert, S. S. Ivanov, N. V. Vitanov, *New J. Phys.* **2009**, *11*, 105051.
- [27] M. Wollenhaupt, T. Baumert, *Faraday Discuss.* **2011**, *153*, 9–26.